Enhanced Catalytic Peroxymonosulfate Activation over Carbon Shell Encapsulating Cobalt Ferrite via Radical and Nonradical Routes

Kaixin Zhu,[a,b,c] Binglian Liang,[c] Changzi Jin,[c] Zoltán Klencsár,[d] Chunxiao Zhao,[b,e] Yanqiang Huang,[c] Ruisheng Hu,[e,] and Junhu Wang[b,c,*]*

[a]*Zhang Dayu School of Chemistry, Dalian University of Technology, Dalian 116024, China*

[b]*Mössbauer Effect Data Center,* [c]*State Key Laboratory of Catalysis, Dalian Institute of Chemical Physics, Chinese Academy of Sciences, Dalian 116023, China*

[d]*Nuclear Analysis and Radiography Department, Institute for Energy Security and Environmental Safety, Centre for Energy Research, Hungarian Academy of Sciences, Konkoly Thege Miklós út 29-33., 1121 Budapest, Hungary.*

[e]*School of Chemistry and Chemical Engineering, Inner Mongolia University, Hohhot 010021, PR China.*

Corresponding Author

**Corresponding author: wangjh@dicp.ac.cn; huruisheng@126.com*

Experimental

Chemicals

Ammonia (25 - 28%) was purchased from Tianjin Kermel Chemical Reagent Company. Resorcinol, ethanol (EtOH), ethylene glycol (> 99%) and cobalt acetate ($Co(CH_3COO)_2 \cdot 4H_2O$) were obtained from Sinopharm Chemical Reagent Co. Ltd. (China). Ferrous acetate ($Fe(CH_3COO)_2$) was supplied by Sigma-Aldrich (USA). Formaldehyde solution (37 - 40%) was purchased from Tianjin Damao Chemical Reagent Company. Orange II sodium salt ($C_{16}H_{11}N_2NaO_4S$) and *tert*-butyl alcohol (TBA) was purchased from Aladdin Chemistry Co. Ltd. PMS, commercially available as Oxone ($2KHSO_5 \cdot KHSO_4 \cdot K_2SO_4$), was purchased from Alfa Aesar. All the chemicals used were of analytical grade and without further treatment, and all the water used was deionized.

Materials synthesis

The synthesis process is depicted in Fig. 1a. RF resin spheres were prepared through the extended Stöber method.[1] After the produced RF polymer spheres were treated by centrifugation, washing and drying, RF-CoFe nanocomposites were synthesized by immersing the spherical RF nanomaterial in the ethylene glycol solution containing cobalt (0.1 mmol) and ferrous (0.2 mmol) acetate precursors through a solvothermal process. Finally, the as-prepared RF-CoFe was calcined in tubular furnace under different atmospheres at 500 ^oC for 4 h with a heating rate of 3 ^oC min^{-1}. The products obtained under atmospheres with various air/Ar (v/v) ratios are denoted as *x*%.

Materials characterization

The X-ray diffraction (XRD) patterns were conducted on a PW3040/60 X'Pert PRO diffractometer (PANalytical) equipped with a copper target (Cu Kα radiation, λ = 1.5406 Å) at an accelerating voltage of 40 kV, a current of 40 mA, and a scanning 2θ range of 10^{o} - 80^{o} at room temperature. The morphology was observed on a field-emission scanning electron microscope (FESEM, JSM-7800F) and a transmission electron microscope (TEM, JEOL JEM-2000). Room temperature (RT) ^{57}Fe Mössbauer spectra[2, 3] were measured on a Topologic 500A spectrometer with ^{57}Co(Rh) as γ-ray radioactive source moving in a constant acceleration mode. The spectra were fitted by using the MossWinn 4.0 program, [4] and ^{57}Fe isomer shift values are given relative to α-iron as a standard. The X-ray photoelectron spectroscopy (XPS) was conducted on a Thermofisher ESCALAB 250Xi instrument with monochromated Al Kα as X-ray source (hν =1486.6eV, 15kV, 10.8mA). The BET surface area and pore distributions were measured on a MicroActive ASAP 2460 instrument. The content of metals in the nanocomposites and the metal leaching of the supernatant after reaction were measured by inductively coupled plasma (ICP) spectrometry on an IRIS Intrepid II XSP instrument. The content of Co was determined by inductively coupled plasma (ICP) for each sample, providing the results of about 5.3 wt%, 5.2 wt%, 15 wt% and 15.6 wt% for the C-CoFe, C-$CoFe_2O_4$, CS-$CoFe_2O_4$ and H-$CoFe_2O_4$, respectively.

Performance evaluation

The performance of catalyst was evaluated through PMS catalytic activation for organics degradation. The experiments were performed in a beaker with Orange II aqueous solution as model dye for degradation at 30 ^{o}C. Typically, 50 mg L^{-1} Orange II aqueous solution and 0.1 g L^{-1} catalyst was added into a 100 mL beaker, followed by stirring for 30 min to obtain the adsorption/desorption equilibrium. The degradation reaction was initiated by adding the PMS oxidant into the above system.

1 mL aqueous solution was withdrawn and immediately quenched by 1 mL ethanol at certain intervals, followed by centrifugation to separate the catalysts. Finally, the supernatant was analyzed by a UV-Vis GBC Cintra apparatus to record the variation of the intensity of absorption peaks at 484 nm for Orange II solution. All the experiments were conducted at least twice. The recycling test was conducted after separating the catalysts after reaction, following by washing and drying. Due to the magnetic property of the catalyst, it can also be separated by magnet (Fig. S8). The used catalyst was regenerated by calcination under inert atmosphere at 400 ^{o}C for 1 h.

The apparent pseudo-first-order reaction rate constants (k) were calculated by the following equation:

$$ln\left(\frac{c_{eq}}{c}\right) = kt \quad (1)$$

where c_{eq} is the concentration of Orange II aqueous solution after adsorption equilibration, c is the real time concentration of Orange II during the reaction, k is the apparent first order rate constant of Orange II removal, and t is the reaction time.

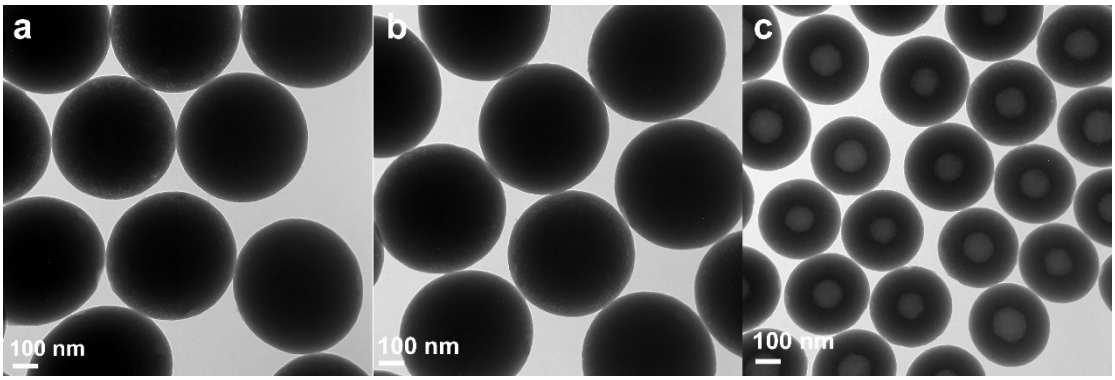

Fig. S1 TEM images of pure RF spheres without cobalt and iron precursors calcined under different atmospheres (a) Ar, (b) 1% air/Ar, (c) 5% air/Ar.

Text S1

Solid carbon spheres were obtained under Ar calcination atmosphere (Fig. S1a). Introduction of very little air (1%) made no significant changes on the obtained carbon spheres, except that the margin of the particles became shallower, and a porous structure appeared around the edge of the spheres (Fig. S1b). However, hollow carbon spheres were successfully formed by further increasing the amount of air to 5% (Fig. S1c), consistent with the phenomenon that we observed on RF-$Co_{0.1}Fe_{0.2}$. Thus, the formation of such hollow carbon spheres is based on the characteristics of RF during calcination.

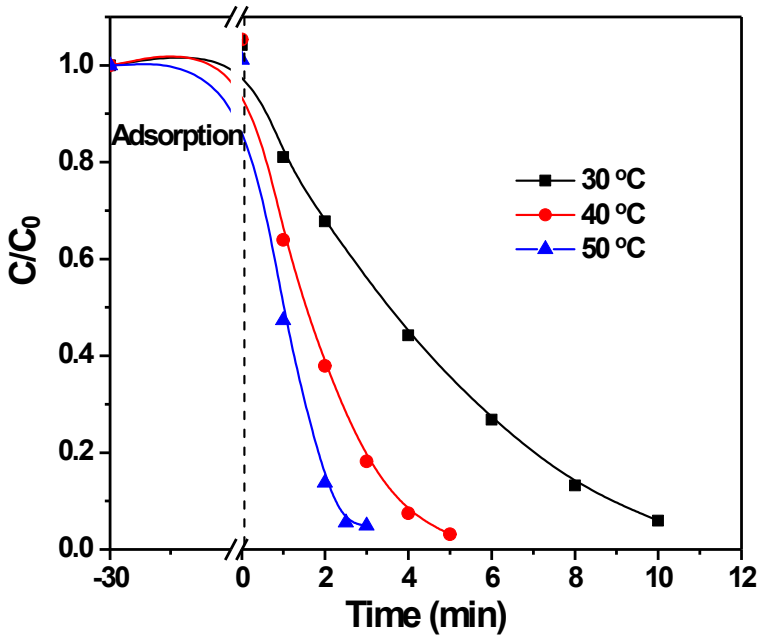

Fig. S2 Effects of solution temperature on the catalytic activity. (Conditions: $[Orange\ II]_0$ = 50 mg L^{-1}; [catalyst] = 0.2 g L^{-1}; [Oxone] = 0.5 g L^{-1}) Under the tested conditions, almost complete removal rate was obtained in 10 min at 30 °C (k = 0.277 min^{-1}, R^2 = 0.98), 5 min at 40 °C (k = 0.707 min^{-1}, R^2 = 0.98) and 3 min at 50 °C (k = 1.147 min^{-1}, R^2 = 0.96), respectively.

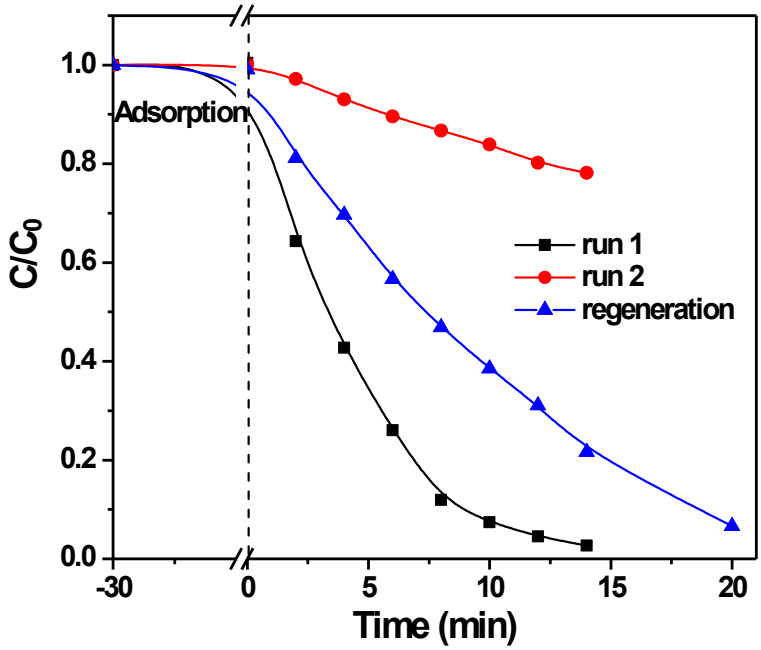

Fig. S3 Recyclability test on the CS-$CoFe_2O_4$ catalyst. (Conditions: $[Orange\ II]_0$ = 50 mg L^{-1}; [catalyst] = 0.1 g L^{-1}; [Oxone] = 0.5 g L^{-1}; T = 30 °C)

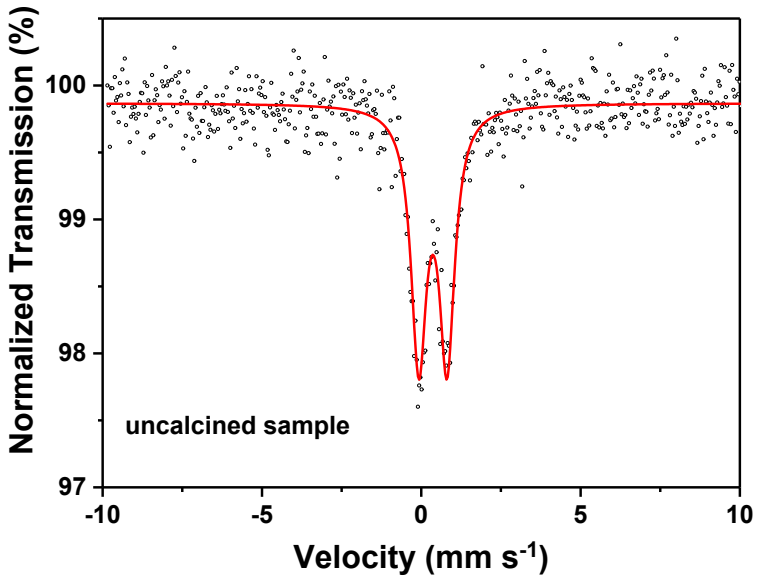

Fig. S4 Mössbauer spectrum of the uncalcined cobalt-iron sample.

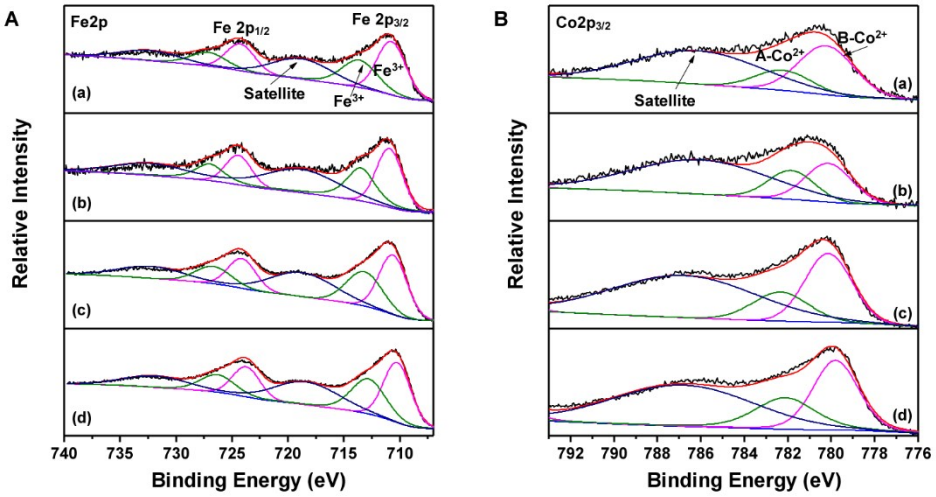

Fig. S5 XPS results of different cobalt-iron catalysts obtained under different atmospheres (a) Ar, (b) 1% air/Ar, (c) 5% air/Ar, (d) air.

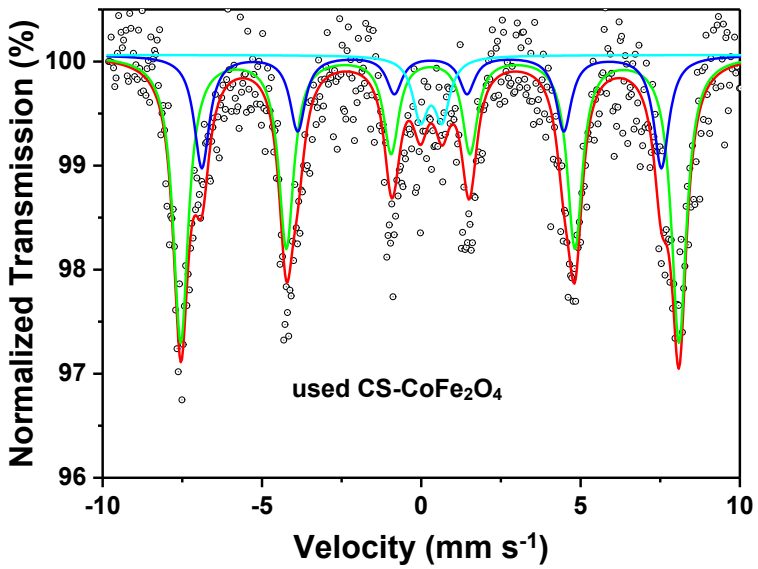

Fig. S6 Mössbauer spectrum of the used CS-$CoFe_2O_4$ catalyst. The catalyst does not alter its iron microenvironments in any significant way, since the obtained respective fit parameters from Mössbauer spectroscopy remain either identical or close to each other for the pristine and the used samples, indicating the good stability of the catalyst.

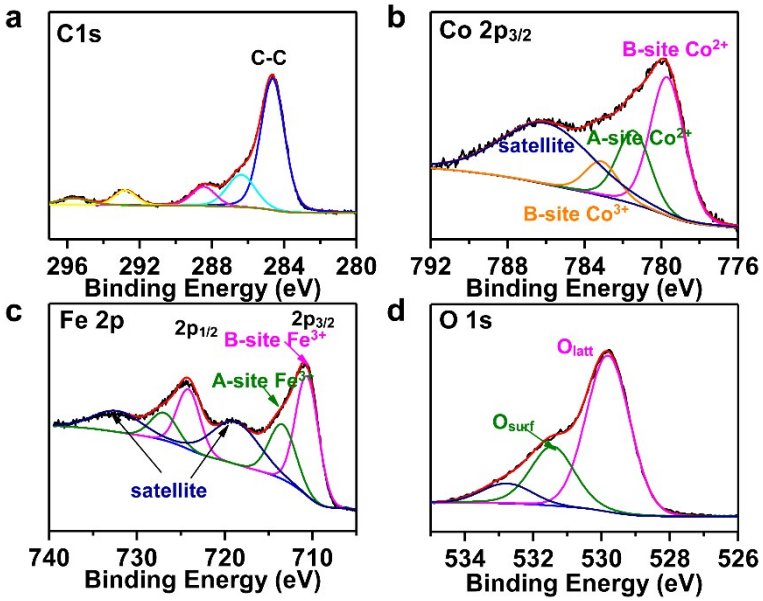

Fig. S7 XPS spectra of the used CS-$CoFe_2O_4$ (a) C1s, (b) Co $2p_{3/2}$, (c) Fe2p, (d) O 1s.

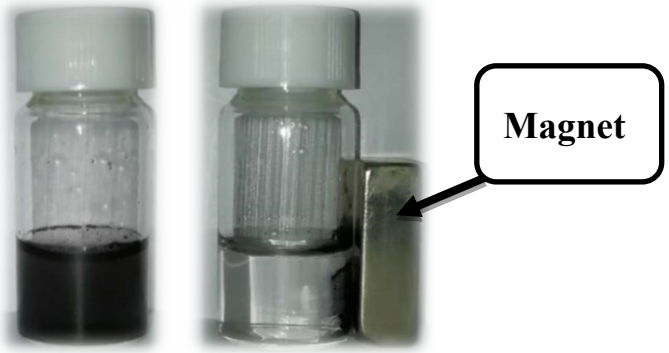

Fig. S8 The photogragh of recovering the catalyst by magnet.

Table S1 Organics degradation via PMS activation of some reported catalysts.

Materials	Organics	Reaction conditions	Degradation	k (min^{-1})	Ref.
Co@N-C **Fe@N-C** **Ni@N-C**	Orange II	[dye] = 20 mg L^{-1}; [catalyst] = 0.02 g L^{-1}; [PMS]/[dye] = 20; T = 25 °C	100% (120 min) 100% (120 min) 47.2% (120 min)	-	5
EDTA-$CoFe_2O_4$	Orange G	[dye] = 100 mg L^{-1}; [catalyst] = 0.2 g L^{-1}; [PMS]/[dye] = 6; T = 25 °C	100% (30 min)	0.152	6
$CoFe_2O_4$/OMC	Rhodamine B	[dye] = 100 mg L^{-1}; [catalyst] = 0.05 g L^{-1}; [PMS]/[dye] = 9; T = 25 °C	100% (60 min)	0.045	7
CoFe/$CoFe_2O_4$	Orange II	[dye] = 60 mg L^{-1}; [catalyst] = 0.05 g L^{-1}; [PMS]/[dye] = 25; T = 20 °C, pH = 7.0	100% (5 min)	0.689	8
Fe_3O_4/Cu(Ni)Cr-LDH	Acid Orange 7	[dye] = 25 mg L^{-1}; [catalyst] = 0.1 g L^{-1}; [PMS]/[dye] = 10; T = 25 °C	100% (30 min)	-	9
Carbon/cobalt/iron	Rhodamine B	[dye] = 10 mg L^{-1}; [catalyst] = 0.05 g L^{-1}; [PMS]/[dye] = 5; T = 30 °C	80% (30 min)	0.098	10
$CoFe_2O_4$	Bisphenol A	[BPA] = 22.8 mg L^{-1}; [catalyst] = 0.2 g L^{-1}; [PMS]/[BPA] = 10; T = 25 °C	96% (60 min)	0.0542	11
$CoFe_2O_4$-GO	Bisphenol A	[BPA] = 22.8 mg L^{-1}; [catalyst] = 0.05 g L^{-1}; [PMS]/[BPA] = 5; T = 20 °C	97% (25 min)	0.330	12
HM-NC@$CoFe_2O_4$	Methylene blue	[MB] = 20 mg L^{-1}; [catalyst] = 0.1 g L^{-1}; [PMS]/[TC] = 8; T = 25 °C	~100% (20 min)	-	13

3D $CoFe_2O_4$/N-rGA	tetracycline	[TC] = 20 mg L^{-1}; [catalyst] = 0.1 g L^{-1}; [PMS]/[TC] = 15; T = 25 °C	93.5% (5 min)	-	[14]
$CoFe_2O_4$@3DG	Benzotriazole	[BTA] = 100 mg L^{-1}; [catalyst] = 0.2 g L^{-1}; [PMS]/[CIP] = 19; T = 23 °C	100% (150 min)	0.0203	[15]
$CoFe_2O_4$/OSC	norfloxacin	[NFC] = 9.6 mg L^{-1}; [catalyst] = 0.5 g L^{-1}; [PMS]/[NFC] = 52; T = 25 °C	90% (60 min)	0.051	[16]
CoFe@NC	4-chlorophenol	[4-CP] = 50 mg L^{-1}; [catalyst] = 0.1 g L^{-1}; [PMS]/[4-CP] = 22; T = 30 °C	99% (30min)	0.241	[17]
CoFe/SiO_2	ciprofloxacin	[CIP] = 10 mg L^{-1}; [catalyst] = 0.2 g L^{-1}; [PMS]/[CIP] = 50; T = 25 °C	98% (5 min)	0.686	[18]
$CoFe_2O_4$@mSiO_2	Orange II	[dye] = 20 mg L^{-1}; [catalyst] = 0.2 g L^{-1}; [PMS]/[dye] = 50; T = 30 °C	93% (35 min)	-	[19]
CS-$CoFe_2O_4$	Orange II	[dye] = 50 mg L^{-1}; [catalyst] = 0.1 g L^{-1}; [PMS]/[dye] = 10; T = 30 °C	98% (14 min)	0.269	This work

Table S2 Apparent reaction rate constants of different catalysts obtained under different calcination atmospheres.

Entry	**C-CoFe**	**C-$CoFe_2O_4$**	**CS-$CoFe_2O_4$**	**H-$CoFe_2O_4$**
k1 (min^{-1})	0.027	0.100	0.269	0.057
k2 ($mg_{Co}^{-1}\cdot min^{-1}$)	0.102	0.385	0.359	0.073
*k3*10³* ($S_{BET}^{-1}\cdot min^{-1}$)	0.080	0.249	6.92	1.18
R^2	0.970	0.982	0.993	0.976

Table S3 Textural Properties of the samples.

samples	**BET surface area ($m^2\ g^{-1}$)**	**pore volume ($cm^3\ g^{-1}$)**	**average pore diameter (nm)**
C-CoFe	336	0.10	7.2
C-$CoFe_2O_4$	401	0.29	6.8
CS-$CoFe_2O_4$	39	0.21	18.0
H-$CoFe_2O_4$	48	0.18	12.4

Table S4 ^{57}Fe Mössbauer parameters obtained by fitting room temperature Mössbauer spectra of cobalt-iron catalysts.

Sample		IS (mm s^{-1})	QS (mm s^{-1})	W_L (mm s^{-1})	Magnetic field (T)	RAF (%)
H-$CoFe_2O_4$	Sextet1	0.303	-0.024	0.582	48.9	67.3
	Sextet2	0.277	-0.006	0.582	45.8	30.8
	Doublet	0.321	0.657	0.582	-	1.9
CS-$CoFe_2O_4$	Sextet1	0.266	-0.028	0.582	48.4	67.1
	Sextet2	0.283	-0.059	0.582	44.6	25.3
	Doublet	0.328	0.660	0.582	-	7.6
C-$CoFe_2O_4$	Doublet	0.333	0.886	0.582	-	-
C-CoFe	Doublet	0.326	0.915	0.582		95.4
	singlet	-0.031	-	0.582		4.6
Used CS-$CoFe_2O_4$	Sextet1	0.282	-0.023	0.577	48.6	66.6
	Sextet2	0.311	0.027	0.582	44.8	26.4
	Doublet	0.314	0.681	0.582	-	7.0
Uncalcined	Doublet	0.364	0.888	0.582	-	-

IS - ^{57}Fe isomer shift relative to α-Fe at room temperature, QS - quadrupole splitting, W_L - Lorentzian FWHM width of absorption peaks, RAF - relative area fraction of the corresponding component,

Table S5 XPS results of the different cobalt-iron samples.

Sample	C1s		O1s		$Co2p_{3/2}$		Fe2p		C/O ratio	Co/Fe ratio	Co atomic (%)
	B.E. (eV)	Percent (%)	B.E. (eV)	Percent (%)	B.E. (eV)	Percent (%)	B.E. (eV)	Percent (%)			
Ar	284.6	74.1	530	37.2	780.2	33.7	710.8	40.4	78/20	0.87	21.3
	286.2	15.4	531.6	29.0	782.2	12.8	713.6	28.0			
	288.8	10.5	533.2	33.8	786.1	52.5	718.8	31.6			
1%	284.6	32.8	530.2	44.6	780.1	22.9	710.9	33.4	75/22	0.79	11.6
air/Ar	286.3	62.1	531.9	41.6	781.8	17.1	713.5	25.8			
	288.8	5.1	533.5	13.8	786	60.0	718.8	40.8			
5%	284.6	68.8	530	68.8	780.1	29.3	710.6	37.4	57/33	0.81	31.1
air/Ar	286	19.8	531.2	29.1	782.3	14.9	713.2	27.6			
	288.4	11.4	532.9	2.1	786.8	55.8	718.7	35.0			
air	284.5	82.5	529.6	81.9	779.8	29.6	710.2	37.1	20/49	0.78	35.0
	286.2	8.5	531.4	18.1	782.1	19.1	712.8	29.4			
	288.1	9.0	-		786.8	51.3	718.4	33.5			
Used	284.6	62.5	529.8	64.2	779.8	23.4	710.6	44.1	30/39	0.71	30.4
5%	286.4	18.1	531.1	26.5	781.7	10.5	713.4	23.5			
air/Ar	288.4	9.1	532.8	9.3	783.4	4.8	718.8	32.4			
	292.8	6.3	-		786.7	61.3	-				
	295.6	4.0	-		-		-				

Supporting References

1 J. Liu, S. Z. Qiao, H. Liu, J. Chen, A. Orpe, D. Zhao and G. Q. Lu, *Angew. Chem. Int. Ed.*, 2011, **50**, 5947-5951.

2 K. Liu, A. I. Rykov, J. H. Wang and T. Zhang, in *Advances in Catalysis, Vol 58*, ed. F. C. Jentoft, Elsevier Academic Press Inc, San Diego, 2015, vol. 58, pp. 1-142.

3 X. N. Li, K. Y. Zhu, J. F. Pang, M. Tian, J. Y. Liu, A. I. Rykov, M. Y. Zheng, X. D. Wang, X. F. Zhu, Y. Q. Huang, B. Liu, J. H. Wang, W. S. Yang and T. Zhang, *Appl. Catal., B*, 2018, **224**, 518-532.

4 Z. Klencsár, *MossWinn manual*, 2016, **59-64**.

5 Y. Yao, H. Chen, C. Lian, F. Wei, D. Zhang, G. Wu, B. Chen and S. Wang, *J Hazard Mater*, 2016, **314**, 129-139.

6 L. Deng, Z. Shi, Z. Zou and S. Zhou, *Environ. Sci. Pollut. Res.*, 2017, **24**, 11536-11548.

7 J. Deng, Y. J. Chen, Y. A. Lu, X. Y. Ma, S. F. Feng, N. Gao and J. Li, *Environ. Sci. Pollut. Res.*, 2017, **24**, 14396-14408.

8 H. Sun, X. Yang, L. Zhao, T. Xu and J. Lian, *J. Mater. Chem. A*, 2016, **4**, 9455-9465.

9 D. Chen, X. Ma, J. Zhou, X. Chen and G. Qian, *J. Hazard. Mater.*, 2014, **279**, 476-484.

10 K.-Y. A. Lin and B.-J. Chen, *Chemosphere*, 2017, **166**, 146-156.

11 C. Cai, S. Kang, X. Xie, C. Liao, X. Duan and D. D. Dionysiou, *J. Hazard. Mater.*, 2020, **399**, 122979.

12 X. Xu, Y. Feng, Z. Chen, S. Wang, G. Wu, T. Huang, J. Ma and G. Wen, *Sep. Purif. Technol.*, 2020, **251**, 117351.

13 T. Zeng, M. Yu, H. Zhang, Z. He, X. Zhang, J. Chen and S. Song, *Sci Total Environ*, 2017, **593-594**, 286-296.

14 F. Ren, W. Zhu, J. Zhao, H. Liu, X. Zhang, H. Zhang, H. Zhu, Y. Peng and B. Wang, *Sep. Purif. Technol.*, 2020, **241**, 116690.

15 X. Li, Z. Liu, Y. Zhu, L. Song, Z. Dong, S. Niu and C. Lyu, *Sci. Total Environ.*, 2020, **749**, 141466.

16 B. Liu, W. Song, H. Wu, Y. Xu, Y. Sun, Y. Yu, H. Zheng and S. Wan, *Chem. Eng. J.*, 2020, **400**, 125947.

17 Y. Zhou, Y. Zhang and X. Hu, *J. Colloid Interface Sci.*, 2020, **575**, 206-219.

18 S. Zhu, Y. Xu, Z. Zhu, Z. Liu and W. Wang, *Chem. Eng. J.*, 2020, **384**.

19 K. Zhu, C. Jin, Z. Klencsár and J. Wang, *Catal. Lett.*, 2017, **147**, 1732-1743.